Photodynamic Therapy Hot Paper

International Edition: DOI: 10.1002/anie.201604781
German Edition: DOI: 10.1002/ange.201604781

Liquid Marbles Based on Magnetic Upconversion Nanoparticles as Magnetically and Optically Responsive Miniature Reactors for Photocatalysis and Photodynamic Therapy

Dan Wang, Lin Zhu, Jian-Feng Chen, and Liming Dai**

Abstract: *Magnetic liquid marbles have recently attracted extensive attention for various potential applications. However, conventional liquid marbles based on iron oxide nanoparticles are opaque and inadequate for photo-related applications. Herein, we report the first development of liquid marbles coated with magnetic lanthanide-doped upconversion nanoparticles (UCNPs) that can convert near-infrared light into visible light. Apart from their excellent magnetic and mechanical properties, which are attractive for repeatable tip opening and magnetically directed movements, the resultant UCNP-based liquid marbles can act as ideal miniature reactors for photodynamic therapy of cancer cells. This work opens new ways for the development of liquid marbles, and shows great promise for liquid marbles based on UCNPs to be used in a large variety of potential applications, such as photodynamic therapy for accelerated drug screening, magnetically guided controlled drug delivery and release, and multifunctional actuation.*

Liquid marbles were first reported by Aussillous and Quéré in 2001[1] and have since attracted tremendous attention.[2] They are usually formed by coating a liquid drop with micro/nanometer-sized superhydrophobic powders, which are often considered as ideal non-wetting systems owing to their hydrophobic surface. To date, a large variety of hydrophobic powders have been used to make various liquid marbles[3] for a range of potential applications, such as electrowetting,[4] micropumping,[5] miniature reactors,[6] gas sensing,[7] and many others.[8] Magnetic liquid marbles based on iron oxide particles show great potential for actuation and manipulation by magnetic forces.[3b,6a,9]

Photon-induced reactions have recently emerged as important processes in chemical and biomedical studies,[10] and some light-responsive liquid marbles have been reported.[6c,11] However, owing to the light absorption and/or scattering by the powder (e.g., graphene,[6c] WO_3 nanoparticles,[11a] TiO_2 nanoparticles,[11b] carbon black)[11c] attached to the droplet surface, visible light can hardly pass through the surface to reach the droplet inside the liquid marble. On the other hand, liquid marbles have been demonstrated to be promising systems for the formation of cancer cell spheroids,[12] which more closely resemble the in vivo physiology of tumors than cells from two-dimensional cell cultures.[13] Furthermore, the use of liquid marbles for the photodynamic therapy (PDT) of cancer cells offers additional advantages for three-dimensional optical emission (irradiation). Nevertheless, conventional liquid marbles are either transparent,[3a,14] but non-magnetic (e.g., silica nanoparticles),[14] or magnetic and opaque (e.g., iron oxide particles),[3b,6a,9] preventing their use in magnetically responsive photon-induced applications. Therefore, the development of magnetic liquid marbles as miniature reactors for photon-induced reactions inside the liquid marbles is challenging.

Lanthanide-doped upconversion nanoparticles (UCNPs), a class of new luminescent nanomaterials that convert two or more low-energy near-infrared (NIR) photons into high-energy photons for UV/Vis emissions, normally consist of transition-metal, lanthanide, or actinide dopant ions embedded in the lattice of an inorganic crystalline host.[15] Thus far, various UCNPs with different host–dopant combinations have been synthesized to generate emissions at different wavelengths.[16] Among them, hexagonal-phase sodium yttrium fluoride ($NaYF_4$) is the most efficient host material for producing green (Yb^{3+}/Er^{3+} co-doped) and blue (Yb^{3+}/Tm^{3+} co-doped) upconversion phosphors.[17] Magnetic UCNPs can also be prepared by doping with Gd^{3+} to obtain optically and magnetically active bifunctional materials for advanced multifunctional devices.[18]

Herein, we describe the preparation of optically and magnetically active bifunctional UCNP-based liquid marbles by doping $NaYF_4$ nanocrystals with $Yb^{3+}/Er^{3+}/Gd^{3+}$ in a facile hydrothermal process. The constituent UCNPs were functionalized with polyhedral oligomeric silsesquioxane (POSS) to make the particles highly hydrophobic,[19] which is required for the formation of liquid marbles. The resultant UCNP-based liquid marbles were exposed to NIR illumination to generate visible emission (i.e., green luminescence) for initiating photoinduced reactions inside the liquid marbles

[*] Dr. D. Wang, Prof. J.-F. Chen
Research Centre of the Ministry of Education for High Gravity Engineering and Technology
State Key Laboratory of Organic-Inorganic Composites
Beijing University of Chemical Technology
Beijing 100029 (China)
E-mail: chenjf@mail.buct.edu.cn
Dr. L. Zhu
Institute of Advanced Materials for Nano-bio Applications
School of Ophthalmology and Optometry
Wenzhou Medical University
270 Xueyuan Xi Road, Wenzhou, Zhejiang (China)
Dr. D. Wang, Dr. L. Zhu, Prof. L. Dai
Center of Advanced Science and Engineering for Carbon (Case4Carbon)
Department of Macromolecular Science and Engineering
Case School of Engineering, Case Western Reserve University
Cleveland, OH 44106 (USA)
E-mail: liming.dai@case.edu

Supporting information for this article can be found under: http://dx.doi.org/10.1002/anie.201604781.

to produce reactive oxygen species (ROS) from protoporphyrin IX (PpIX),[10a,b] followed by photodynamic therapy of cancer cells in situ. Thus this work describes a novel application for liquid marbles and a new approach for photodynamic therapy.

The $Yb^{3+}/Er^{3+}/Gd^{3+}$-doped $NaYF_4$ upconversion nanoparticles were synthesized by well-developed hydrothermal synthetic methods using oleic acid as the surfactant.[20] According to a previously reported procedure,[20a] the Yb^{3+}, Er^{3+}, and Gd^{3+} dopant concentrations in the UCNPs were adjusted to 18, 2, 50 mol%, respectively, to obtain nanoparticles with a highly crystalline hexagonal phase for efficient upconversion luminescence. Figure 1b shows a typical transmission electron microscopy (TEM) image of the resultant UCNPs, which reveals the average size of the UCNPs to be 100–200 nm in length and 20–50 nm in width. The presence of surface carboxyl groups on the UCNP nanoparticles allowed for further surface modification with amino-functionalized POSS molecules by amide formation to form hydrophobic UCNP-POSS nanoparticles (Figure 1a). The UCNP/POSS weight ratio in the UCNP-POSS nanoparticles was determined by thermogravimetric analysis (TGA) to be about 3:1 (Figure 1c). As can be seen in the Supporting Information, Figure S6, a UCNP-POSS film showed superhydrophobicity with an air/water contact angle (CA) as high as 151°, a value that is even higher than that for POSS films (123°), which is beneficial for the formation of liquid marbles. Owing to the high concentration of Gd^{3+} dopant in the UCNPs, the UCNP-POSS nanoparticles were magnetic (Figure S9). These results suggest the possible use of UCNP-POSS nanoparticles for the encapsulation of aqueous droplets to form magnetic liquid marbles (see below).

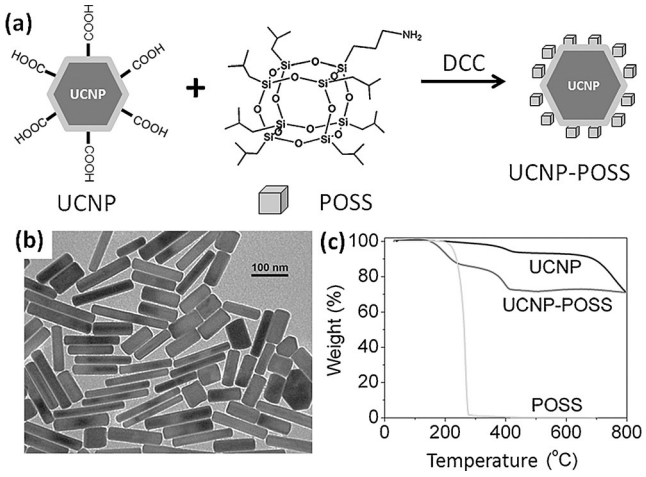

Figure 1. a) Synthesis of POSS-grafted UCNP (UCNP-POSS) nanoparticles. b) A typical TEM image of the UCNP nanoparticles. c) TGA of UCNP, POSS, and UCNP-POSS. DCC = dicyclohexylcarbodiimide.

As schematically shown in Figure 2, the liquid marbles were prepared simply by rolling water droplets on a pile of UCNP-POSS particles owing to their high hydrophobicity. As the water droplet is rolled over, the UCNP-POSS nanoparticles spontaneously self-organize in a process that is driven by the capillary forces[2b] at the water/air interface to encapsulate the water droplet and render the droplet non-wetting to the substrate. Subsequently, more UCNP-POSS nanoparticles are adsorbed on the surface of the liquid marble to form UCNP-POSS multilayers (Figure 2a). Figure 2b shows a typical digital photograph of a liquid marble with a diameter of about 1.5 mm prepared from 3 μL water, which could roll freely on the surface of a glass dish (see the Supporting Information for a Movie). The excellent stability of the liquid marble further enabled it to be readily handled with a pair of tweezers without breaking (Figures 2c and S10). Figure 2d shows that the liquid marble remained intact after being transferred onto a water surface in a Petri dish. The weight ratio of the UCNP-POSS powder and the inner water molecules was gravimetrically measured to be 1:9. The upconversion liquid marble can be opened and closed reversibly or actuated to move in different directions under a magnetic field owing to its magnetic nature (Figure 2e, f; see also Figure S9). For ease of visualization, a liquid marble containing red-colored water (containing cell-culture medium, see below) was used in Figure 2e for the demonstration of the magnetic-field-induced tip opening. The ability to undergo magnetic-field-induced opening could enable the opened liquid surface to wet a contacting glass capillary, and it could thus be used for transferring liquid into or out of the liquid marble (Figure S11). Figure 2f shows the motion of a liquid marble placed on a water surface (the same liquid marble shown in Figure 2d) under a magnetic field. The direction of movement of the liquid marble changed in response to the motion of the external magnet.

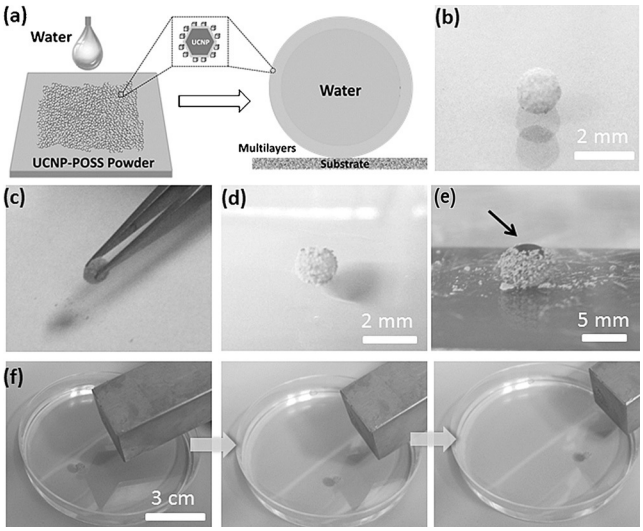

Figure 2. a) Formation of a liquid marble by rolling a water droplet on UCNP-POSS powder. Digital photographs of b) a liquid marble made from water and UCNP-POSS powder (droplet size: 3 μL), c) a liquid marble being picked up with a pair of tweezers, d) a liquid marble placed on a water surface, and e) a magnetically opened liquid marble. f) Snapshots showing the controlled movement of a liquid marble floating on a water surface in response to an external magnetic field.

Another remarkable feature of the UCNP-POSS nanoparticles is their upconversion luminescence. For traditional liquid marbles (e.g., iron oxide based liquid marbles), visible

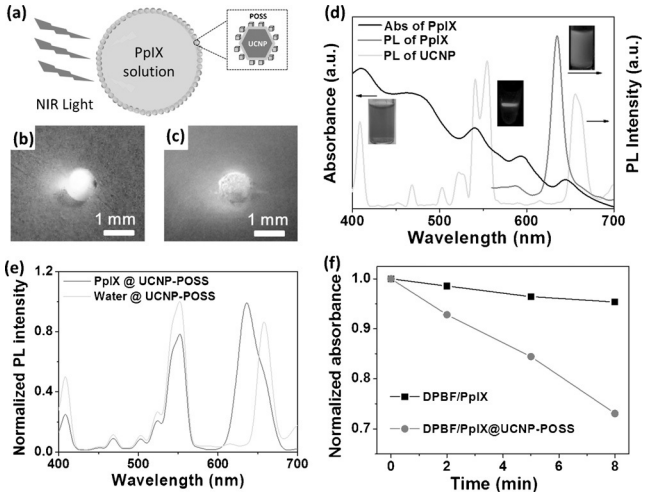

Figure 3. a) Illustration of a liquid marble encapsulating PpIX solution under NIR laser irradiation. Photographs of a liquid marble encapsulating b) pure water and c) PpIX solution under NIR laser irradiation. d) Photoluminescence spectrum of the as-prepared UCNPs excited with a 980 nm laser and absorbance and photoluminescence spectra of the as-prepared PpIX solution. Insets: Pictures of a PpIX solution in water, the photoluminescence of a UCNP solution in chloroform, and the photoluminescence of PpIX solution in water (from left to right). e) Photoluminescence spectra of liquid marbles encapsulating pure water and PpIX solution. f) Normalized decay curves of the absorption density at $\lambda = 410$ nm for a DPBF/PpIX mixture in a tube (optical glass 10 mm cell cuvette) and a UCNP-POSS liquid marble encapsulating PpIx for four different times of irradiation with a 980 nm laser beam (normalized by the absorbance intensity at $t = 0$ min).

light can hardly pass through the outer layer of the liquid marble owing to the strong absorption and scattering of light by the solid particle coating (Figure S12). For the UCNP-POSS-based liquid marble, however, the UCNP outer layer, after doping with Yb^{3+} and Er^{3+} for converting two or more low-energy NIR photons into high-energy photons (e.g., green emission), could act as a light transducer to introduce high-energy photons (i.e., UV/Vis emission) into the liquid marble for photocatalysis. To identify the photon conversion ability of the UCNP liquid marbles, we performed NIR-light-induced photocatalysis of protoporphyrin IX (PpIX) inside the liquid marble (Figure 3a). PpIX can be excited to generate reactive oxygen species (ROS) from endogenous oxygen upon irradiation with light of an appropriate wavelength (Figure S13). Figure 3 shows photographs of liquid marbles encapsulating pure water (b) and PpIX solution (c) under NIR laser irradiation. A liquid marble formed from water and UCNP-POSS exhibited green color under NIR laser excitation (Figure 3b) whereas a liquid marble obtained from a PpIX solution and UCNP-POSS powder gave yellow emission under the same conditions (Figure 3c). The luminescence spectrum of as-prepared UCNPs under NIR excitation ($\lambda = 980$ nm), along with the absorbance and photoluminescence spectra of a PpIX solution, is shown in Figure 3d. The luminescence peak positions of the UCNPs match well with the absorbance peaks of PpIX, promoting the excitation of PpIX. The photoluminescence spectra of liquid marbles encapsulating pure water and PpIX solution are shown in Figure 3e. The photoluminescence spectrum of a liquid marble with pure water is similar to that of UCNP-POSS with intensive green luminescence (peak at $\lambda = 550$ nm). For the liquid marble with PpIX solution, the green luminescence (peak at $\lambda = 550$ nm) decreased in intensity with a concomitant enhancement of red luminescence (peak at $\lambda = 630$ nm), indicating the excitation of PpIX by the upconversion luminescence from UCNP-POSS under NIR irradiation. The generation of ROS was indirectly confirmed with 1,3-diphenylisobenzofuran (DPBF) as a chemical probe, whose absorbance at $\lambda = 410$ nm decreases in the presence of ROS. Figure 3f shows the normalized decay curves of the absorption density at $\lambda = 410$ nm for PpIX in a DPBF/PpIX mixture and a UCNP-POSS-based liquid marble as a function of time under irradiation with a 980 nm laser beam. The absorption of the DPBF in the UCNP-POSS-based liquid marbles showed a much stronger time dependence than that of the DPBF/PpIX mixture, indicating more efficient ROS generation for the former (see also Figure S15). As the luminescence wavelength of the UCNPs is tunable from the UV to the NIR range by doping with various lanthanide ions, the upconversion liquid marble can be used as a miniature reactor for photocatalysis over the whole NIR–UV spectrum.

Liquid marbles have recently been used for the formation of cancer cell spheroids[12] as the three-dimensional cell cultures in liquid marbles more closely resemble the in vivo physiology of tumors than two-dimensional cell cultures.[13] For the first time, we performed a study on the photodynamic therapy of cancer cells by incubating cells inside the UCNP liquid marbles, along with PpIX as a ROS generator, and using the upconversion nanoparticle coating to provide the required irradiation (Figure 4a). Figures 4b shows a digital photograph of a liquid marble formed from an aqueous suspension of MAD-MD-231 cells (200 μL) and UCNP-POSS

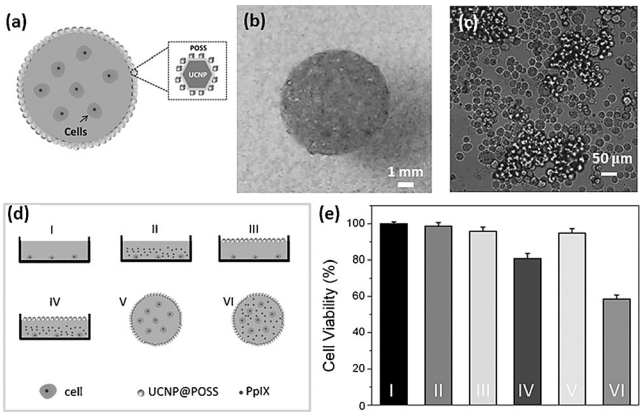

Figure 4. a) Schematic representation of a cell-encapsulating liquid marble. Digital photographs of liquid marble(s) based on UCNP-POSS powder and cell culture media (drop size 200 μL) b) without and c) with encapsulated MAD-MD-231 cells. d) Schematic representations of cells in culture dishes without PpIX (I), with PpIX (II), without PpIX but with UCNP-POSS powder (III), with both PpIX and UCNP-POSS powder (IV), and of cells in a liquid marble without PpIX (V) and with PpIX (VI). e) Cell viability of the cells in (d) after irradiation with a 980 nm laser (1 $W cm^{-2}$) for 4 min.

powder, and Figure 4c shows an optical microscopy image of MAD-MD-231 cells. Apart from the photodynamic therapy of cells inside the liquid marbles, control experiments were also carried out, in which cells were cultured in normal culture dishes with and without PpIX and/or UCNP-POSS nanoparticles (Figure 4d). MTT studies were then performed to determine the cell viabilities (Figure S16). To investigate the distribution of cells within the liquid marble, the UCNP-POSS powder from a deliberately broken cell-encapsulating liquid marble was imaged with an optical microscope. No cells were observed in the UCNP-POSS powder from the broken liquid marble (Figure S17), suggesting that the cells were well-dispersed inside the liquid marble rather than sedimented on or stuck to the inner surface of the UCNP-POSS shell. Figure S18 gives the results from the MTT test for the MAD-MD-231 cells inside the liquid marbles with and without PpIX, which showed decreased cell viability with increasing exposure time to a 980 nm laser in the presence of PpIX, indicating NIR-induced photodynamic therapy of the cancer cells. For the cells inside the liquid marbles without PpIX, however, NIR light irradiation had no significant effect on cell viability. In control experiments, NIR exposure under the same conditions caused a decrease in cell viability for the MAD-MD-231 cells in the culture dish with both PpIX and UCNP-POSS powder (IV in Figures 4d,e), but not for the same cells inside culture dishes that do not contain both PpIX and UCNP-POSS powder (I–III in Figures 4d,e). Owing to the large contact area between the UCNP-POSS powder coating and the cell culture media as well as the spherical geometry to enable 360° irradiation, the PpIX-encapsulating UCNP-based liquid marbles exhibited a much more efficient photodynamic therapy compared to the same treatment performed with the two-dimensional culture dishes (sample VI vs. IV in Figures 4d,e). Both cells incubated with UCNP-POSS powder in a culture dish (III) and cells incubated in a liquid marble without PpIX (V) exhibited high viability, demonstrating that the marble shell material had low toxicity. Therefore, the observed reduced cell viability in sample VI could be confidently attributed to the photodynamic therapy. Although these preliminary results on photodynamic therapy of cancer cells inside the UCNP liquid marbles could be further improved by optimizing the experimental conditions (e.g., the liquid marble size/shell thickness, the cell and/or drug concentrations, and the irradiation intensity), these results clearly indicate that liquid marbles based on upconversion nanoparticles provide important advantages for biomedical studies, particularly for accelerating drug screening for the photodynamic therapy of cancer cells.

In summary, we have described the advantages of using lanthanide-doped upconversion nanoparticles as encapsulating powders to prepare optically and magnetically active bifunctional liquid marbles. By chemical bonding of POSS to the surface of $Yb^{3+}/Er^{3+}/Gd^{3+}$-doped $NaYF_4$ UCNPs, we prepared superhydrophobic UCNP-POSS composite nanoparticles as coatings for the formation of liquid marbles from water droplets. The resultant liquid marbles based on UCNP-POSS and water exhibited excellent mechanical stability, magnetic properties, and were able to convert low-energy near-infrared photons into high-energy UV/Vis photons. These unique properties, in combination with the associated three-dimensional cell cultures and three-dimensional optical emission (irradiation), render these UCNP-based liquid marbles ideal miniature reactors for studying the photodynamic therapy of cancer cells inside the liquid marbles with NIR irradiation. We believe that liquid marbles based on UCNPs show great promise for a large variety of applications, including, but not limited to, photodynamic therapy for accelerated drug screening, magnetically controlled drug delivery and release, and multifunctional actuation.

Acknowledgements

We are grateful for financial support from WMU-CWRU (SPN2330), the NSF (CMMI-1400274), and partial support from the Fundamental Research Funds for the Central Universities (BUCTRC201601), and the "111" project of China (B14004).

Keywords: liquid marbles · magnetic properties · nanoparticles · photodynamic therapy · upconversion

How to cite: *Angew. Chem. Int. Ed.* **2016**, *55*, 10795–10799
Angew. Chem. **2016**, *128*, 10953–10957

[1] P. Aussillous, D. Quéré, *Nature* **2001**, *411*, 924–927.
[2] a) P. Aussillous, D. Quéré, *Proc. R. Soc. London Ser. A* **2006**, *462*, 973–999; b) G. McHale, M. I. Newton, *Soft Matter* **2011**, *7*, 5473–5481; c) E. Bormashenko, *Curr. Opin. Colloid Interface Sci.* **2011**, *16*, 266–271; d) G. McHale, M. I. Newton, *Soft Matter* **2015**, *11*, 2530–2546.
[3] a) P. S. Bhosale, M. V. Panchagnula, H. A. Stretz, *Appl. Phys. Lett.* **2008**, *93*, 034109; b) Y. Zhao, J. Fang, H. Wang, X. Wang, T. Lin, *Adv. Mater.* **2010**, *22*, 707–710; c) L. Zhang, D. Cha, P. Wang, *Adv. Mater.* **2012**, *24*, 4756–4760; d) V. Sivan, S.-Y. Tang, A. P. O'Mullane, P. Petersen, N. Eshtiaghi, K. Kalantar-zadeh, A. Mitchell, *Adv. Funct. Mater.* **2013**, *23*, 144–152; e) E. Bormashenko, Y. Bormashenko, R. Grynyov, H. Aharoni, G. Whyman, B. P. Binks, *J. Phys. Chem. C* **2015**, *119*, 9910–9915; f) W. Wei, R. Lu, W. Ye, J. Sun, Y. Zhu, J. Luo, X. Liu, *Langmuir* **2016**, *32*, 1707–1715.
[4] G. McHale, D. L. Herbertson, S. J. Elliott, N. J. Shirtcliffe, M. I. Newton, *Langmuir* **2007**, *23*, 918–924.
[5] E. Bormashenko, R. Balter, D. Aurbach, *Appl. Phys. Lett.* **2010**, *97*, 091908.
[6] a) Y. Xue, H. Wang, Y. Zhao, L. Dai, L. Feng, X. Wang, T. Lin, *Adv. Mater.* **2010**, *22*, 4814–4818; b) T. Arbatan, L. Li, J. Tian, W. Shen, *Adv. Healthcare Mater.* **2012**, *1*, 80–83; c) W. Gao, H. K. Lee, J. Hobley, T. Liu, I. Y. Phang, X. Y. Ling, *Angew. Chem. Int. Ed.* **2015**, *54*, 3993–3996; *Angew. Chem.* **2015**, *127*, 4065–4068; d) Y. Sheng, G. Sun, T. Ngai, *Langmuir* **2016**, *32*, 3122–3129.
[7] a) J. F. Tian, T. Arbatan, X. Li, W. Shen, *Chem. Commun.* **2010**, *46*, 4734–4736; b) J. Tian, T. Arbatan, X. Li, W. Shen, *Chem. Eng. J.* **2010**, *165*, 347–353; c) Z. Xu, Y. Zhao, L. Dai, T. Lin, *Part. Part. Syst. Charact.* **2014**, *31*, 839–842.
[8] a) H. K. Lee, Y. H. Lee, I. Y. Phang, J. Wei, Y.-E. Miao, T. Liu, X. Y. Ling, *Angew. Chem. Int. Ed.* **2014**, *53*, 5054–5058; *Angew. Chem.* **2014**, *126*, 5154–5158; b) Y. Sheng, G. Sun, J. Wu, G. Ma, T. Ngai, *Angew. Chem. Int. Ed.* **2015**, *54*, 7012–7017; *Angew. Chem.* **2015**, *127*, 7118–7123; c) M. C. Serrano, S. Nardecchia, M. C. Gutiérrez, M. L. Ferrer, F. D. Monte, *ACS Appl. Mater. Interfaces* **2015**, *7*, 3854–3860; d) R. K. Vadivelu, C. H. Ooi,

R. Q. Yao, J. T. Velasquez, E. Pastrana, J. Diaz-Nido, F. Lim, J. Ekkberg, N. T. Nguyen, J. St John, *Sci. Rep.* **2015**, *5*, 15083.
[9] Y. Zhao, Z. Xu, H. Niu, X. Wang, T. Lin, *Adv. Funct. Mater.* **2015**, *25*, 437 – 444.
[10] a) J. Qian, D. Wang, F. Cai, Q. Zhan, Y. Wang, S. He, *Biomaterials* **2012**, *33*, 4851 – 4860; b) Y. Zhang, J. Qian, D. Wang, Y. Wang, S. He, *Angew. Chem. Int. Ed.* **2013**, *52*, 1148 – 1151; *Angew. Chem.* **2013**, *125*, 1186 – 1189; c) X. Lang, J. Zhao, X. Chen, *Angew. Chem. Int. Ed.* **2016**, *55*, 4697 – 4700; X. Lang, J. Zhao, X. Chen, *Angew. Chem.* **2016**, *128*, 4775 – 4778; d) F. Yang, J. Koeller, L. Ackermann, *Angew. Chem. Int. Ed.* **2016**, *55*, 4759 – 4762; *Angew. Chem.* **2016**, *128*, 4837 – 4840.
[11] a) X. Tang, S.-Y. Tang, V. Sivan, W. Zhang, A. Mitchell, K. Kalantar-zadeh, K. Khoshmanesh, *Appl. Phys. Lett.* **2013**, *103*, 174104; b) T. T. Y. Tan, A. Ahsan, M. R. Reithofer, S. W. Tay, S. Y. Tan, T. S. A. Hor, J. M. Chin, B. K. J. Chew, X. Wang, *Langmuir* **2014**, *30*, 3448 – 3454; c) M. Paven, H. Mayama, T. Sekido, H.-J. Butt, Y. Nakamura, S. Fujii, *Adv. Funct. Mater.* **2016**, *26*, 3199 – 3206.
[12] T. Arbatan, A. Al-Abboodi, F. Sarvi, P. P. Y. Chan, W. Shen, *Adv. Healthcare Mater.* **2012**, *1*, 467 – 469.
[13] a) W. Mueller-Klieser, *Am. J. Physiol.* **1997**, *273*, C1109 – C1023; b) J. A. Hickman, R. Graeser, R. de Hoogt, S. Vidic, C. Brito, M. Gutekunst, H. van der Kuip, *Biotechnol. J.* **2014**, *9*, 1115 – 1128.
[14] a) G. Sun, Y. Sheng, T. Ngai, *Soft Matter* **2016**, *12*, 542 – 545; b) X. Li, Y. Xue, P. Lv, H. Lin, F. Du, Y. Hu, J. Shen, H. Duan, *Soft Matter* **2016**, *12*, 1655 – 1662.
[15] a) F. Wang, X. Liu, *Chem. Soc. Rev.* **2009**, *38*, 976 – 989; b) M. Haase, H. Schäfer, *Angew. Chem. Int. Ed.* **2011**, *50*, 5808 – 5829; *Angew. Chem.* **2011**, *123*, 5928 – 5950; c) G. Chen, H. Qiu, P. N. Prasad, X. Y. Chen, *Chem. Rev.* **2014**, *114*, 5161 – 5214.
[16] a) Q. Q. Zhan, J. Qian, H. J. Liang, G. Somesfalean, D. Wang, S. L. He, Z. G. Zhang, S. Andersson-Engels, *ACS Nano* **2011**, *5*, 3744 – 3757; b) M. Yang, Y. Liang, B. Zhao, Q. Gui, M. Lin, L. Yan, H. You, L. Dai, Y. Liu, D. Jin, *Sci. Rep.* **2015**, *5*, 11844; c) W. Zheng, P. Huang, D. Tu, E. Ma, H. Zhu, X. Chen, *Chem. Soc. Rev.* **2015**, *44*, 1379 – 1415.
[17] a) K. W. Krämer, D. Biner, G. Frei, H. U. Güdel, M. P. Hehlen, S. R. Luthi, *Chem. Mater.* **2004**, *16*, 1244 – 1251; b) J. F. Jin, Y. J. Gu, C. W. Y. Man, J. P. Cheng, Z. H. Xu, Y. Zhang, H. S. Wang, V. H. Y. Lee, S. H. Cheng, W. T. Wong, *ACS Nano* **2011**, *5*, 7838 – 7847; c) J. Zhou, Q. Liu, W. Feng, Y. Sun, F. Li, *Chem. Rev.* **2015**, *115*, 395 – 465.
[18] a) J. Zhou, M. Yu, Y. Sun, X. Zhang, X. Zhu, Z. Wu, D. Wu, F. Li, *Biomaterials* **2011**, *32*, 1148 – 1156; b) Y. X. Liu, D. S. Wang, J. X. Shi, Q. Peng, Y. D. Li, *Angew. Chem. Int. Ed.* **2013**, *52*, 4366 – 4369; *Angew. Chem.* **2013**, *125*, 4462 – 4465.
[19] a) E. Ayandele, B. Sarkar, P. Alexandridis, *Nanomedicine* **2012**, *2*, 445 – 475; b) B. Duan, H. Gao, M. He, L. Zhang, *ACS Appl. Mater. Interfaces* **2014**, *6*, 19933 – 19942; c) D. Wang, J. Liu, J.-F. Chen, L. Dai, *Adv. Mater. Interfaces* **2016**, *3*, 1500439.
[20] a) X. Wang, J. Zhuang, Q. Peng, Y. Li, *Nature* **2005**, *437*, 121 – 124; b) F. Wang, Y. Han, C. S. Lim, Y. Lu, J. Wang, J. Xu, H. Chen, C. Zhang, M. Hong, X. Liu, *Nature* **2010**, *463*, 1061 – 1065.

Received: May 16, 2016
Revised: June 27, 2016
Published online: August 3, 2016

